Journal of
Materials Chemistry A

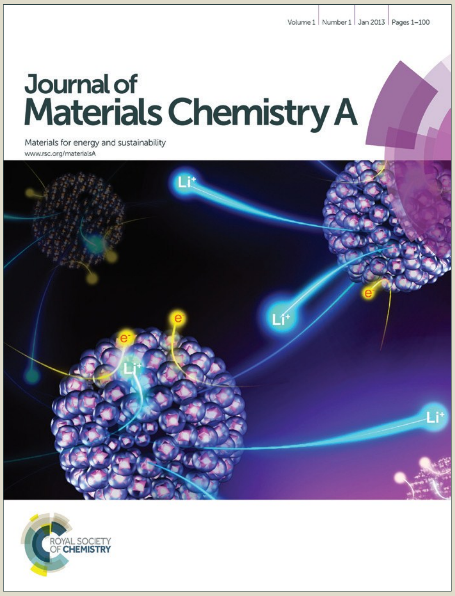

ROYAL SOCIETY
OF CHEMISTRY

www.rsc.org/materialsA

Journal of Materials Chemistry A

COMMUNICATION

Li^+ interstitials as the charge carriers in superionic lithium-rich anti-perovskites

Received 00th January 20xx,
Accepted 00th January 20xx

DOI: 10.1039/x0xx00000x

www.rsc.org/MaterialsA

R. Mouta,[a] E. M. Diniz[a] and C. W. A. Paschoal*[a,b]

Here, we report that in lithium-rich anti-perovskites (LiRAPs) with lithium halide deficiency, Li^+ interstitials outnumber vacancies by 2-3 orders of magnitude, so that interstitials might be the actual charge carriers responsible for superionic conduction, as opposed to what has been assumed so far. This finding has important implications and may be crucial to an efficient tailoring of LiRAPs, aiming their commercial use as safe electrolytes in all-solid-state lithium-ion batteries.

Nowadays, lithium ion batteries (LIBs) are widely used in portable electronic devices such as cell phones and laptops. However, safety issues related to the flammable liquid electrolytes employed still restrict their broad-scale use in large systems, such as electric vehicles.[1,2] Although the replacement of liquid electrolytes by solid ones could overcome this issue, their low Li^+ conductivity has been a limiting factor.

Out of the several materials proposed recently as solid electrolytes for LIBs,[3–6] a new family of Li-based solid electrolytes with anti-perovskite structure[7] whose chemical formula is Li_3OA (A = halogen) has been intensively investigated,[2,7–17] emerging as a strong candidate to overcome such limitation. In addition to their superionic conductivity, these lithium-rich anti-perovskites (LiRAPs) also exhibit good cyclability,[2] a wide electrochemical window (larger than 5 eV),[2,8,9] good structural stability up to 540-550 K,[2,7] low electronic conductivity,[2] low activation enthalpy, low cost and lightweight. Besides, they are non-flammable, recyclable and environmentally friendly, being suitable for commercial use,[2,7] inclusive in lithium-air batteries and with metallic lithium anode.[2,11]

Among LiRAPs, the bulk crystalline samples with highest ionic conductivity reported so far are those presenting LiA deficiency.[7] It has been assumed that such strong LiA deficiency degrees (up to 20%) induce high concentrations of A^- and Li^+ vacancies, the latter being the charge carriers responsible for the superionic conductivity,[7,11] as A^- vacancies are expected to have very low mobility. Li^+ interstitials have also been considered as charge carriers, for having much higher mobility in LiRAPs than Li^+ vacancies,[9,13] but it was already shown that Frenkel defects have high formation energy at 0 K,[9] while a previous investigation from our group revealed that Li^+ interstitials concentration due to Frenkel defects in Li_3OCl is lower than 10^{-13} even near the melting point.[13] Thus, it has been argued that interstitials from Frenkel defects cannot account for superionic conductivity.[9,13,14] Accordingly, interpretation of results and efforts to improve ionic conductivity have been based strictly on a Li^+ vacancy-driven transport mechanism.[7,11,14] Nevertheless, while Frenkel defects are the only possible origin of Li^+ interstitials in either stoichiometric or divalent cation-doped LiRAPs, LiA deficiency, on the other hand, may potentially give rise to Li^+ interstitials, as pointed out by Emly *et al*,[9] bringing back the possibility of an interstitial transport mechanism as the responsible for the superionic conductivity.

We point out that several evidences support an interstitial mechanism over a vacancy one in LiA-deficient LiRAPs. For example, experimental values of migration enthalpy from LiA-deficient samples are appreciably lower than theoretical ones for vacancy migration,[7–9,13] while agree well with theoretical values for interstitial migration.[9,13] In addition, experimental values of migration enthalpy obtained from divalent cation doped samples (in which the charge carriers are necessarily Li^+ vacancies, due to charge compensation)[2] differ significantly from those of LiA-deficient samples,[7] indicating distinct conductive processes. Also, ionic conductivity calculated at 300 K with molecular dynamics,[8] assuming only Li^+ vacancies as charge carriers is in good agreement with the extrapolated experimental value for stoichiometric samples,[2] but is one order of magnitude below the experimental value for LiA-deficient samples, although Li^+ vacancies concentration used in calculations (4.17%) had the same order of magnitude (6.66%)

---

[a] Departamento de Física, Universidade Federal do Maranhão, São Luís, Maranhão, 65080-805, Brazil.
[b] Departamento de Física, Universidade Federal do Ceará, Fortaleza, Ceará, 60020-181, Brazil. E-mail: paschoal.william@fisica.ufc.br

† Electronic Supplementary Information (ESI) available: computational technical details, numeric data from defect calculations and statistical physics calculation of the ratio between interstitials and vacancies. See DOI: 10.1039/x0xx00000x

as in the most LiA-deficient samples.[7,8] Finally, *ab initio* calculations showed that A^- vacancies hampers Li^+ vacancies transport, increasing their migration enthalpy,[8] while experimental migration enthalpies for LiA-deficient samples are actually very low.[7]

However, as LiA deficiency can, in principle, yield to creation of either Li^+ vacancies or interstitials, an important question still remains: for a fixed degree of LiA deficiency, which charge carriers are actually created, vacancies or interstitials? In other words, are Li^+ interstitials present in such a high concentration to account for superionic conductivity in LiA-deficient LiRAPs? Once atomistic level modelling based on interionic potentials is a well-established and reliable tool for assessing defect energetics in LIB materials,[13,18–23] we used it (technical details in Atomistic Modelling section, ESI†),[24–26] to elucidate this question by calculating the lattice Gibbs energy of Li_3OCl in each of these two alternative pictures assuming the same degree δ of non-stoichiometry ($LiCl:Li_2O=1-\delta$) for both, with the lowest energy configuration being the most stable one.

In the first one (LiCl deficiency picture), the adequate chemical formula is $Li_{3-\delta}OCl_{1-\delta}$ and, for each LiCl unit absent compared to the number of Li_2O units involved in the synthesis procedure, one Li^+ vacancy and one Cl^- vacancy are created (Fig. 1a). The synthesis reaction is:[7]

$$Li_2O + (1-\delta)LiCl \rightarrow Li_{3-\delta}OCl_{1-\delta}\ , \qquad (1)$$

in which (Kröger-Ving notation was used for defects)[27]

$$Li_{3-\delta}OCl_{1-\delta} \equiv Li_3OCl + \delta \cdot (v'_{Li} + v^{\cdot}_{Cl})\ . \qquad (2)$$

In the other (Li_2O excess picture), some of the sites that should ideally be occupied by ions from LiCl units are in fact occupied with ions from Li_2O units, with O^{2-} replacing Cl^- at perovskite's A-site, one of Li^+ ions standing in its regular position and the extra Li^+ taking an interstitial position (Fig. 1b), so that chemical formula is best written as $Li_{3+\alpha}O_{1+\alpha}Cl_{1-\alpha}$ or $Li_{3+\alpha}O(Cl_{1-\alpha}O_\alpha)$, with the synthesis reaction being:

$$(1+\alpha)Li_2O + (1-\alpha)LiCl \rightarrow Li_{3+\alpha}O_{1+\alpha}Cl_{1-\alpha}\ , \qquad (3)$$

in which

$$Li_{3+\alpha}O_{1+\alpha}Cl_{1-\alpha} \equiv Li_3OCl + \alpha \cdot (Li^{\cdot}_i + O'_{Cl})\ . \qquad (4)$$

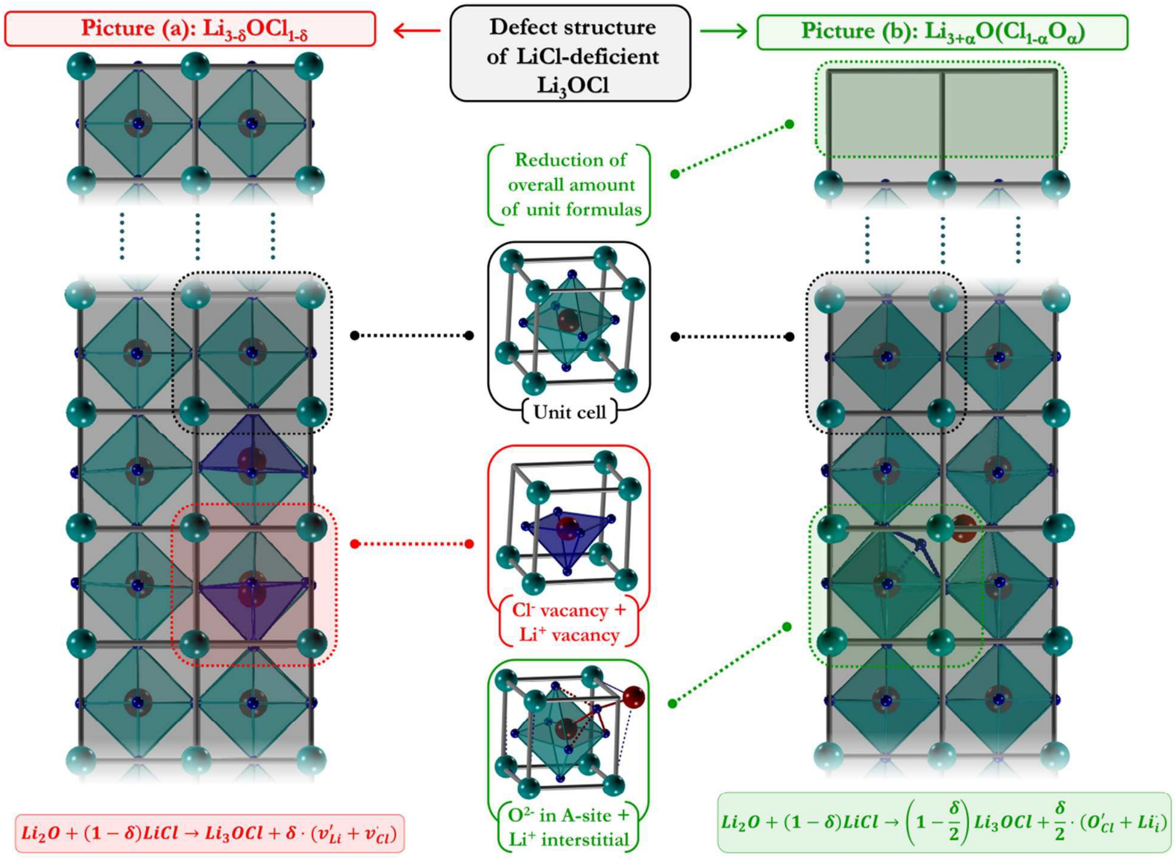

Fig. 1 The two possible pictures that can give rise to lithium charge carriers in Li_3OCl due to partial depletion of LiCl during synthesis procedure. Li^+, O^{2-} and Cl^- are represented by dark blue, red and cyan spheres, respectively. In picture (a), LiCl deficiency leads to formation of Li^+ and Cl^- vacancies, as shown in the central inset in red. In picture (b), Li_2O excess leads to the replacement of some Cl^- ions by O^{2-} ions and to formation of Li^+ interstitials, preferentially assuming the configuration shown in the lower inset in green. The Li_2O units spent in this process, along with other LiCl units lacking (since they are outnumbered by Li_2O units), result in depletion of material to build new unit cells and the consequent volume and number of unit cells reduction, as shown in the upper green inset. The bulk regions shown at the right and left sides are lateral views of the most favorable configurations in each picture, calculated using 2x2x4 supercells (configurations obtained using other supercell dimensions were identical). The lower boxes show the synthesis reaction in each case, with the reduction of unit formulas due to building material depletion becoming explict in picture (b).

For appropriate comparison, we must renormalize this reaction to match the reactants amount and ratio as in Eq. (1):

$$Li_2O + (1-\delta)LiCl \rightarrow (1-0.5\delta)Li_{3+\alpha}O_{1+\alpha}Cl_{1-\alpha}\,, \qquad (5)$$

with

$$\delta = 2\alpha/(1+\alpha)\,. \qquad (6)$$

Now comparing Eq. (5) with Eq. (1) and using Eq. (4), we get the equation analogue to Eq. (2), representing the defect structure in this picture:

$$Li_{3-\delta}OCl_{1-\delta} \equiv (1-0.5\delta)Li_3OCl + 0.5\delta\cdot(Li_i^{\cdot} + O'_{Cl})\,. \qquad (7)$$

From this equation, it becomes evident that for each two absent LiCl units one only Li^+ interstitial is formed, and the overall number of unit cells is reduced by one. This reduction is expected, since part of the Li_2O that would otherwise be used as building material for new cells is now used to fill in for part of the absent LiCl.

From Eq. (2) and Eq. (7) we obtained the lattice Gibbs energy per unit formula of $Li_{3-\delta}OCl_{1-\delta}$ for each picture (dashed lines in Fig. 2) based on lattice Gibbs energy per unit formula of the stoichiometric crystal and on Gibbs energy of the corresponding defects in the limit of infinite dilution (see Table S1, ESI†). Such energies depend on crystal's temperature and should be taken right before the melting point, *ca.* 550 K. After all, once we lower the temperature (*e.g.*, the cooling process after the sample is removed from furnace), even if the most favourable configuration is reversed and is no longer the same as at the melting point, the mobilities of Cl^- and O^{2-} ions are expected to be low enough to avoid such radical change from one type of microscopic configuration to another. Therefore, all calculations were performed at 550 K.

Supercell calculations (solid spheres in Fig. 2) were also performed, as they take explicitly into account interactions between defects, thus showing better reliability in the high concentration limit. We used 2x2x2, 2x2x4, 3x3x3 and 4x4x4 supercells, with one vacancy (interstitial) per supercell, corresponding to the following values of δ for LiCl deficiency (Li_2O excess) picture: 1/8 (2/9), 1/16 (2/17), 1/27 (1/14) and 1/64 (2/65). The values in parentheses were obtained through Eq. (6). In both calculation methods the most energetically favourable configuration always corresponded to bounded defects at nearest-neighbour distances (see central insets in green and red in Fig. 1), with Gibbs energy increasing monotonically the larger the distance between defects – a behaviour also observed at Emly *et al.*'s defect calculations performed at 0 K using supercells.[9] Thus all values used in Fig. 2 correspond to nearest-neighbour bound defects.

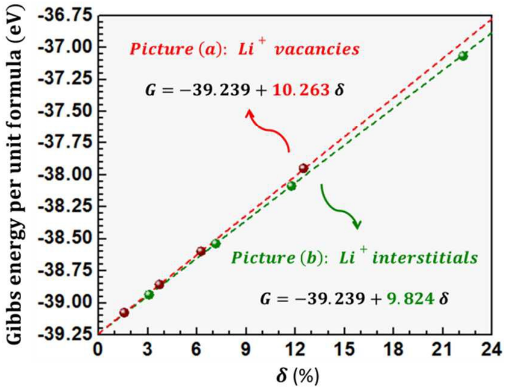

Fig. 2 Gibbs energy dependence of $Li_{3-\delta}OCl_{1-\delta}$ on the degree of LiCl deficiency for both pictures. The dashed lines were obtained from Eq. (2) and Eq. (7), using the data in Table S1, while solid spheres were obtained from supercell calculations, using the data in Table S2 and S3.

We note in Fig. 2 an excellent agreement between lattice Gibbs energies calculated using the two methods, which means that, in this case, calculating Gibbs energies without taking into account the interaction between like defects is a very good approximation, even for δ > 20%. The reason for this is that the only interaction between like defects is the electrostatic one, since the remaining are short-ranged. As we considered neutral pairs of defects, the electrostatic contribution from positively charged defects cancel that from negatively charged defects.

Most importantly, we observe from Fig. 2 that the configuration in which interstitials are the charge carriers is the most energetically favourable one over the entire range of LiCl deficiency degrees investigated. Despite the apparent small Gibbs energy difference between the two pictures per unit formula, this difference is large for macroscopic samples, reaching *ca.* 8.5 kJ for 1 mol of unit formulas when δ = 20%.

To help visualizing the correct significance of this Gibbs energy difference, Fig. 3 shows the ratio between the number of interstitials and vacancies in a more flexible picture where both previous pictures are allowed to coexist. This ratio was calculated from a statistical physics analysis (details in Statistical Physics Analysis section, ESI†) by assuming that the LiCl-deficient crystal is at thermodynamic equilibrium, which implies that its Gibbs energy must assume a minimum value. Such analysis led to the following expression for the ratio between the number of interstitials and vacancies at 550 K, which is dependent on the degree of deficiency δ:

$$n_i/n_v = 3.042\times 10^3\,\sqrt{\delta/(2-\delta)}\,. \qquad (8)$$

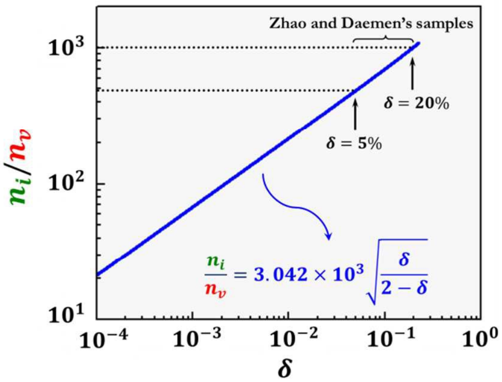

Fig. 3 Ratio between the number of lithium interstitials and vacancies. The range of LiCl deficiency in samples synthesized by Zhao and Daemen (5% ≤ δ ≤ 20%) is also shown.[7]

We observe that, even at LiCl deficiency degrees as low as 1%, the number of interstitials is more than 200 times greater than the number of vacancies, this ratio reaching values over 1000/1 at 20%. Consequently, the appropriate formula is $Li_{3+\alpha}O(Cl_{1-\alpha}O_{\alpha})$, with samples being actually denser than stoichiometric ones. More importantly, taking into account that vacancies have much lower mobility than interstitials,[9,13] for all practical purposes the contribution of vacancies to ionic conduction might be in fact be negligible in heavily LiCl-deficient samples, as those synthesized by Zhao and Daemen.[7]

Conclusions

Here, we demonstrated that Li^+ interstitials outnumber Li^+ vacancies by 2-3 orders of magnitude in heavily LiCl-deficient Li_3OCl, so that interstitials, not vacancies, shall be the charge carriers responsible for superionic conduction. We suggest this behavior is not limited to Li_3OCl, but holds for halide-deficient LiRAPs in general, as strongly supported by several aforementioned evidences. This is the opposite of what has been assumed so far, and gives not only a reinterpretation to transport mechanisms in LiA-deficient LiRAPs, but also new insights to efficient tailoring of LiRAPs in general. For example, LiA deficiency might be a more efficient tailoring technique for increasing Li^+ conductivity than aliovalent cation doping, once Li^+ interstitials are significantly more mobile than vacancies.[9,13] In addition, LiA-deficient samples simultaneously doped with aliovalent cations may not present conductivity improvement over LiA-deficient only samples, due to possible annihilation between Li^+ vacancies and interstitials, which must be further investigated. Thus, our finding is of great importance to define which procedures can be used to boost even more the conductivity in LiRAPs, aiming an efficient development of safer LIBs. Besides, theoretical techniques used here have quite general validity and can be easily applied for many other similar ionic materials, e.g. NaRAPs, the related sodium-rich anti-perovskites that have been recently proposed as solid electrolytes for all-solid state sodium-ion batteries.[28]

Acknowledgements

This study was partially supported by Brazilian funding agencies CAPES and CNPq. We are grateful to Dr. J. D. Gale for permission of use of GULP code. R. Mouta thanks Drs. E. N. Silva and E. F. V. Carvalho for providing computer facilities and MSc. D. A. B. Barbosa for suggestions on the manuscript.

Notes and references

1 N.-S. Choi, Z. Chen, S. A. Freunberger, X. Ji, Y.-K. Sun, K. Amine, G. Yushin, L. F. Nazar, J. Cho and P. G. Bruce, *Angew. Chem. Int. Ed. Engl.*, 2012, **51**, 9994–10024.
2 M. H. Braga, J. A. Ferreira, V. Stockhausen, J. E. Oliveira and A. El-Azab, *J. Mater. Chem. A*, 2014, **2**, 5470.
3 C. Cao, Z. Li, X. Wang, X. Zhao and W. Han, *Front. Energy Res.*, 2014, **2**, 1–10.
4 N. Kamaya, K. Homma, Y. Yamakawa, M. Hirayama, R. Kanno, M. Yonemura, T. Kamiyama, Y. Kato, S. Hama, K. Kawamoto and A. Mitsui, *Nat. Mater.*, 2011, **10**, 682–686.
5 S. Stramare, V. Thangadurai and W. Weppner, *Chem. Mater.*, 2003, 15, 3974–3990.
6 Y. Deng, C. Eames, J.-N. Chotard, F. Lalère, V. Seznec, S. Emge, O. Pecher, C. P. Grey, C. Masquelier and M. S. Islam, *J. Am. Chem. Soc.*, 2015, **137**, 9136–9145.
7 Y. Zhao and L. L. Daemen, *J. Am. Chem. Soc.*, 2012, **134**, 15042–7.
8 Y. Zhang, Y. Zhao and C. Chen, *Phys. Rev. B*, 2013, **87**, 134303.
9 A. Emly, E. Kioupakis and A. Van der Ven, *Chem. Mater.*, 2013, **25**, 4663–4670.
10 D. J. Schroeder, A. A. Hubaud and J. T. Vaughey, *Mater. Res. Bull.*, 2014, **49**, 614–617.
11 X. Lü, G. Wu, J. W. Howard, A. Chen, Y. Zhao, L. L. Daemen and Q. Jia, *Chem. Commun. (Camb).*, 2014, **50**, 11520–2.
12 J. Zhang, J. Han, J. Zhu, Z. Lin, M. H. Braga, L. L. Daemen, L. Wang and Y. Zhao, *Inorg. Chem. Commun.*, 2014, **48**, 140–143.
13 R. Mouta, M. Á. B. Melo, E. M. Diniz and C. W. A. Paschoal, *Chem. Mater.*, 2014, **26**, 7137–7144.
14 Z. Deng, B. Radhakrishnan and S. P. Ong, *Chem. Mater.*, 2015, **27**, 3749–3755.
15 J. Zhang, J. Zhu, L. Wang and Y. Zhao, *Chem. Commun.*, 2015, **51**, 9666–9669.
16 M.-H. Chen, A. Emly and A. Van der Ven, *Phys. Rev. B*, 2015, **91**, 214306.
17 L. Ye, L. Wang, H. Xie, Y. Su, X. Jin and C. Zhang, *Energy Technol.*, 2015, n/a–n/a.
18 E. Gonzalo, A. Kuhn, F. García-Alvarado and M. S. Islam, *J. Mater. Chem. A*, 2013, **1**, 6588.
19 C. A. J. Fisher, N. Kuganathan and M. S. Islam, *J. Mater. Chem. A*, 2013, **1**, 4207.
20 C. Eames, J. M. Clark, G. Rousse, J.-M. Tarascon and M. S. Islam, *Chem. Mater.*, 2014, **26**, 3672–3678.
21 P. M. Panchmatia, A. R. Armstrong, P. G. Bruce and M. S. Islam, *Phys. Chem. Chem. Phys.*, 2014, **16**, 21114–21118.
22 J. Roos, C. Eames, S. M. Wood, A. Whiteside and M. Saiful Islam, *Phys. Chem. Chem. Phys.*, 2015, **17**, 22259–22265.
23 M. S. Islam and C. A. J. Fisher, *Chem. Soc. Rev.*, 2014, **43**, 185–204.
24 J. D. Gale, *J. Chem. Soc.{,} Faraday Trans.*, 1997, **93**, 629–637.
25 J. D. Gale and A. L. Rohl, *Mol. Simul.*, 2003, **29**, 291–341.
26 J. D. Gale, *Zeitschrift für Krist. - Cryst. Mater.*, 2005, **220**, 552–554.
27 F. A. Kröger and H. J. Vink, *Solid State Phys. - Adv. Res. Appl.*, 1956, **3**, 307–435.
28 Y. Wang, Q. Wang, Z. Liu, Z. Zhou, S. Li, J. Zhu, R. Zou, Y. Wang, J. Lin and Y. Zhao, *J. Power Sources*, 2015, **293**, 735–740.